JOURNAL OF Materials CHEMISTRY

Structural characterization of Li α-sialon ceramics by high-resolution ^{27}Al and ^{29}Si NMR spectroscopy

Pierre Kempgens,[a] Robin K. Harris,*[a] Zhengbo Yu[b] and Derek P. Thompson[b]

[a]*Department of Chemistry, University of Durham, South Road, Durham, UK DH1 3LE. E-mail: r.k.harris@durham.ac.uk*
[b]*Department of Mechanical, Materials and Manufacturing Engineering, The University, Newcastle upon Tyne, UK NE1 7RU*

Received 7th March 2001, Accepted 24th July 2001
First published as an Advance Article on the web 7th September 2001

High-resolution ^{29}Si and ^{27}Al NMR spectra have been obtained from seven crystalline samples of lithium α-sialon with different compositions. The ^{29}Si isotropic chemical shift is found to be constant within the experimental error across the whole substitution range and its value, $\delta_{Si} \approx -48$ ppm, suggests that silicon remains largely in an SiN_4 coordination for all compositions. The ^{27}Al 1D MAS NMR spectra exhibit a range of tetrahedral coordinations AlO_xN_{4-x} ($x = 0$–4), which vary as the aluminium and oxygen contents increase. The results are consistent with previous studies of sialons, which indicate that silicon prefers to be coordinated by nitrogen whereas aluminium prefers coordination by oxygen. Some NMR parameters are derived from two-dimensional ^{27}Al MQMAS spectra, including those for the resolved AlO_4 peak. However, it is shown that this technique does not allow the different aluminium tetrahedral mixed environments (AlO_3N, AlO_2N_2 and $AlON_3$) to be resolved.

Introduction

The term ''sialons'' is used to describe phases in the Si–Al–O–N and M–Si–Al–O–N (M = metal) systems. Of the many such phases that have been characterised, the α- and β-forms are the most important from both scientific and technological points of view.[1–3] These compounds have three-dimensional structures composed of $(Si,Al)O_xN_{4-x}$ ($0 \leqslant x \leqslant 4$) tetrahedra. In β-sialons, aluminium and oxygen substitute for silicon and nitrogen to give a solid solution of the type $Si_{6-z}Al_zO_zN_{8-z}$, where $0 < z < 4$. α-Sialons[4] are formed from α-Si_3N_4 by partial replacement of Si^{4+} by Al^{3+}, with valency compensation being achieved by inserting modifier cations (Li, Ca, Y and most Ln) into the interstices of the (Si,Al)–N network. Some oxygen atoms also replace nitrogen atoms, and α′-phases therefore have a general composition of the type $M_xSi_{12-(m+n)}Al_{m+n}O_nN_{16-n}$ where $x \leqslant 2$ because there are only two available interstitial sites per unit cell, and m(Al–N) plus n(Al–O) bonds replace $(m+n)$(Si–N) bonds in the unit cell of α-Si_3N_4. The M cations occupy the large interstices in the structure.

High-resolution solid-state NMR has proved to be a powerful technique for probing the short-range structure and chemistry of materials, particularly when phase mixtures of crystalline and amorphous components are present. It is particularly valuable compared to conventional diffraction techniques such as X-ray diffraction (XRD) for aluminosilicates and oxynitride ceramics because of the similarity in scattering factors for the pairs of atoms aluminium/silicon and oxygen/nitrogen. The technique of magic-angle spinning (MAS) has been used to distinguish different silicon and aluminium local coordinations by their isotropic chemical shifts. Local coordination units which have been identified in ceramics by ^{29}Si and ^{27}Al MAS NMR include SiO_xN_{4-x} ($x = 0$–4), AlN_4, AlO_4, AlO_5 and AlO_6.[5–16] By contrast to what happens in the case of spin $I = 1/2$ nuclei such as ^{29}Si, the ^{27}Al nucleus (spin $I = 5/2$) has an electric quadrupole moment which interacts with surrounding electric field gradients, arising from non-spherical charge distributions around the nucleus. Normally only the central ($1/2 \leftrightarrow -1/2$) transition is observed as it is free of quadrupolar effects to first order and affected only by the much smaller second-order quadrupolar interaction. Although MAS can average out the first-order interactions, this technique is not able to completely cancel the second-order quadrupolar interaction. Recently, a new two-dimensional multiple-quantum MAS NMR technique (MQMAS) has been proposed by Frydman and Harwood,[17] which yields high-resolution spectra for half-integer quadrupolar nuclei. This method usually allows the determination of the isotropic chemical shift and electric field gradient (efg) tensor components *via* analysis of the line positions along the two dimensions.

In the present work ^{27}Al MAS and 2D 3Q MAS NMR techniques are applied to examine seven Li α-sialon samples, $Li_mSi_{12-(m+n)}Al_{m+n}O_nN_{16-n}$ (*i.e.* $x = m$) with different m, n values, as indicated in Table 1. For the purposes of comparison, the compositions are all given such that the atom counts of Si and Al add to 12, but samples are listed in order of decreasing N : O ratio. We regard the N : Si ratio as particularly significant (it correlates with the amount of Li present and is not influenced by the presence of AlO_6 in glassy domains), so this is also to be found in Table 1. The 2D 3Q MAS NMR experiment may be useful to identify the different aluminium sites and to determine the isotropic chemical shift as well as the efg tensor components which characterize each of these sites. It has been shown[16] that mixed aluminium tetrahedral coordinations of the type AlO_xN_{4-x} ($x = 1$–3) are found for β′-sialons, giving ^{27}Al shifts in the range between 60 ppm (which corresponds to the shift of AlO_4 coordination) and 110 ppm (which corresponds to the shift of AlN_4 coordination). It is of interest to know if such mixed units also form in Li α′-sialons and if better resolution can be obtained by the use of the MQMAS NMR technique compared to that of conventional MAS NMR. In this work, we clearly show the existence of such mixed units. In addition, the results obtained by ^{29}Si MAS NMR will be presented.

DOI: 10.1039/b102168k

Table 1 Aluminium-27 isotropic chemical shifts and second-order quadrupolar effect parameters for the Li α-sialon samples

Sample no.	Compound	N : O	N : Si	δ_{MAS}[a]/ppm	δ_1[a]/ppm	δ_{Al}/ppm	λ[b]/MHz	Assignment[c]
I	$Li_{1.3}Si_{9.5}Al_{2.5}O_{1.2}N_{14.8}$	12.3	1.56	87	106	97	3.2	"AlO_2N_2"
				53	58	56	1.6	AlO_4
II	$Li_{1.69}Si_{9.0}Al_{3.0}O_{1.31}N_{14.69}$	11.2	1.63	90	103	97	2.6	"AlO_2N_2"[d]
				54	66	60	2.5	AlO_4
III	$Li_{1.0}Si_{9.5}Al_{2.5}O_{1.5}N_{14.5}$	9.7	1.53	85	106	96	3.3	"AlO_2N_2"
				54	64	59	2.4	AlO_4
				−1	6	3	1.9	AlO_6
IV	$Li_{2.0}Si_{8.5}Al_{3.5}O_{1.5}N_{14.5}$	9.7	1.71	93	102	98	2.1	"AlO_2N_2"[d]
V	$Li_{1.0}Si_{9.0}Al_{3.0}O_{2.0}N_{14.0}$	7.0[e]	1.56	92	100	96	2.1	"AlO_2N_2"
				55	57	56	1.2	AlO_4
				3	15	9	2.6	AlO_6
VI	$Li_{2.0}Si_{7.5}Al_{4.5}O_{2.5}N_{13.5}$	5.4	1.80	91	102	97	2.4	"AlO_2N_2"[d]
				54	57	56	1.4	AlO_4
				0	10	5	2.3	AlO_6
VII	$Li_{1.0}Si_{8.5}Al_{3.5}O_{2.5}N_{13.5}$	3.9[e]	1.59	94	111	103	3.0	"AlO_2N_2"
				2	13	7	2.4	AlO_6

[a]δ_{MAS} and δ_1 are the centres of gravity in the two dimensions of the MQMAS spectra. [b]Second-order quadrupolar effect parameter, see eqn. (2). [c]"AlO_2N_2" includes AlO_3N, $AlON_3$ and (probably) AlN_4 environments. [d]Includes a substantial amount of a high-frequency signal which can probably be assigned to AlN_4. [e]Probably somewhat higher in the crystalline domains since a substantial amount of the AlO_6 environment is detected, presumably from glassy regions.

Experimental

A. Sample preparation

The compositions investigated lie on the α-sialon plane defined by the formula $Li_mSi_{12-(m+n)}Al_{m+n}O_nN_{16-n}$. The synthesis of these samples has been described in a recent publication.[18] Even though the compositions have been calculated to lie exactly in the α-sialon plane, it is common to find that additional oxygen has been incorporated into the mix during milling due to hydrolysis of the starting nitride powders. It is therefore expected that some residual Li–Si–Al–O–N glass will remain in the samples after processing.

B. NMR measurements

Silicon-29 MAS NMR spectra were collected at $B_0 = 7.05$ T on a Varian Unity Plus spectrometer operating at 59.583 MHz. A Doty probe was used, samples were packed in a 7 mm ZrO_2 rotor, and the spin rate was in the range 3.4–3.6 kHz. All experiments used a single π/2 pulse excitation (6 μs duration), a rf field strength of 42 kHz (as determined *via* a sample of solid tetra(trimethylsilyl)methane), a 300 s recycle delay and a spectral width of 30 kHz. The ^{29}Si spectra generally required between 160 and 288 transients each. The spectra were referenced to the ^{29}Si resonance of an external sample of solid tetra(trimethylsilyl)methane at $\delta_{Si} = -1.4$ ppm with respect to the conventional shift reference of TMS.

The ^{27}Al 1D MAS and 2D 3Q MAS NMR experiments were carried out using a Chemagnetics Infinity-600 spectrometer ($B_0 = 14.1$ T). The corresponding ^{27}Al Larmor frequency is 156.384 MHz. For both 1D and 2D 3Q MAS experiments, a standard 3.2 mm Chemagnetics MAS probe with a MAS frequency of 20 kHz was used. For obtaining the ^{27}Al 1D MAS spectra a single-pulse excitation of 1 μs, corresponding to a π/10 flip angle, and a recycle delay of 250 ms were used. No saturation effects have been observed. For each sample, 2048 transients were added. The 2D 3Q MAS experiments were carried out using the three-pulse phase-modulated split-t_1 experiment proposed by Wimperis and Brown.[19,20] The experiment makes use of the more efficient $|\Delta p| = 2$ triple- to single-quantum conversion compared to the $|\Delta p| = 4$ one, which means that, in contrast to the optimum spin $I = 3/2$ experiment, the two parts of the t_1 period are separated by the spin-echo interval. The main advantage of this experiment is that no shearing of the data is required as the whole echo is acquired. A rf field strength of $\nu_{rf} \approx 156$ kHz was used, as determined using a 1.0 M $AlCl_3 \cdot 6H_2O$ aqueous solution. The duration of the triple-quantum excitation pulse was 2.45 μs, while those of the $p = +3$ to $p = +1$ transfer pulse and of the $p = +1$ to $p = -1$ conversion pulse were 0.8 μs. Typically, 1632 transients consisting of 256 points each were added for each of the 128 increments of t_1, and the recycle delay was 200 ms. The t_1 increments ranged from 4 to 10 μs and the duration of the spin-echo interval was typically 1 ms. The ^{27}Al chemical shifts, reported in parts per million, were determined relative to an aqueous external sample of 1.0 M $AlCl_3 \cdot 6H_2O$ by replacement.

The 1D spectra only yield apparent ^{27}Al chemical shifts, which will be denoted here as δ'_{Al}. The standard procedure[21–25] for 2D MQMAS spectra is to measure the positions of the centres of gravity (with respect to the reference frequency) $\Delta\nu_{MAS}$ and $\Delta\nu_1$ along the MAS and isotropic dimensions, respectively. It has been shown that these values can be used to determine the true (isotropic) chemical shift δ_{Al} of a given aluminium site, using eqn. (1), adapted from refs. 22 and 23 for the case of a spin-$^5/_2$ nucleus:

$$\delta_{Al} = 10^6(16\Delta\nu_1 + 15\Delta\nu_{MAS})/31\nu_0 \quad (1)$$

where ν_0 is the ^{27}Al Larmor frequency. The second-order quadrupolar effect parameter, which we denote by λ, is then given by eqn. (2), adapted from ref. 25:

$$\lambda^2 = \chi^2\left(1 + \frac{\eta_Q^2}{3}\right) = 2000(\Delta\nu_1 - \Delta\nu_{MAS})\nu_0/93 \quad (2)$$

where χ is the quadrupolar coupling constant ($= e^2qQ/h$) and η_Q the asymmetry parameter of the electric field gradient tensor. Discrimination among the exact contributions of χ and η_Q to the shifts in both dimensions is usually carried out by analyzing the powder lineshapes which can be resolved from the 2D MQMAS spectrum for each chemical site. However, one usually requires well-defined lineshapes such as typical second-order quadrupolar powder patterns.[26] In this work, the lineshapes that can be extracted from the 2D 3Q MAS spectra are featureless and it is therefore not possible to determine accurately the NMR parameters (isotropic shift, quadrupolar coupling constant and asymmetry parameter of the efg tensor) by this method. Another procedure to extract the NMR parameters involves the fit of the full MAS NMR spectrum using as starting parameters those that can be deduced from the analysis of the line positions along the two dimensions.[27] However, this method requires the knowledge of the population of each site when several sites are present in the sample. Again, this was not feasible in the present work. Therefore, this work is limited to the analysis of the line positions in both dimensions. Since $0 \leqslant \eta_Q \leqslant 1$, the ratio of the highest to the

lowest possible value of $|\chi|$ in eqn. (2) is 1.15, so that, determining λ gives a good estimation of $|\chi|$. The isotropic chemical shift and the second-order quadrupolar effect parameter have been obtained for each site in the following way: the shift $\Delta\nu_1$ was obtained for each site from the projection of the 2D 3Q MAS spectrum in the isotropic dimension. Then for each site at its $\Delta\nu_1$ shift, a slice was taken in the MAS dimension and $\Delta\nu_{MAS}$ (the centre of gravity of that MAS lineshape) was determined using an in-house computer program, freq MQ. From the values of $\Delta\nu_1$ and $\Delta\nu_{MAS}$, one deduces $\Delta\nu_{Al}$ and λ using eqns. (1) and (2). The isotropic chemical shifts δ_{Al} and second-order quadrupolar effect parameters η that can be deduced from the analysis of the line positions in the two dimensions are given in Table 1. These are believed to be accurate to *ca.* ± 2 ppm and ± 0.3, respectively.

Results

Because the compounds studied in this work have different compositions, the ^{27}Al experimental results can be presented in several ways, but in Table 1 and Figs. 1–3 the order is in terms of increasing oxygen content (decreasing N : O ratio). Another possible way would be in terms of increasing aluminium content, which would place the samples in the order I, III, V, II, VII, IV, VI. This order is also used in part of the discussion. First, the spectrum of each compound will be briefly described. The data extracted from the ^{27}Al MQMAS results are given in Table 1.

Sample I: $Li_{1.3}Si_{9.5}Al_{2.5}O_{1.2}N_{14.8}$ ($m = 1.3$; $n = 1.2$)

Fig. 1 shows the ^{27}Al MAS and 3Q MAS NMR spectra of this sample. The 1D spectrum exhibits a narrow line at

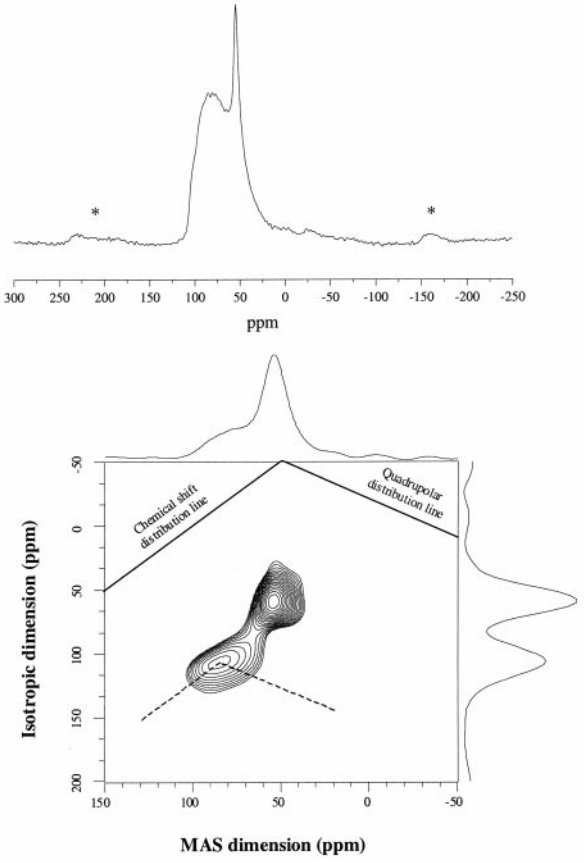

Fig. 1 Aluminium-27 1D MAS (top) and 2D 3Q MAS (bottom) NMR spectra of sample I ($Li_{1.3}Si_{9.5}Al_{2.5}O_{1.2}N_{14.8}$) recorded at $B_0 = 14.1$ T and $\nu_r = 20$ kHz. Asterisks on the 1D MAS spectrum correspond to spinning sidebands.

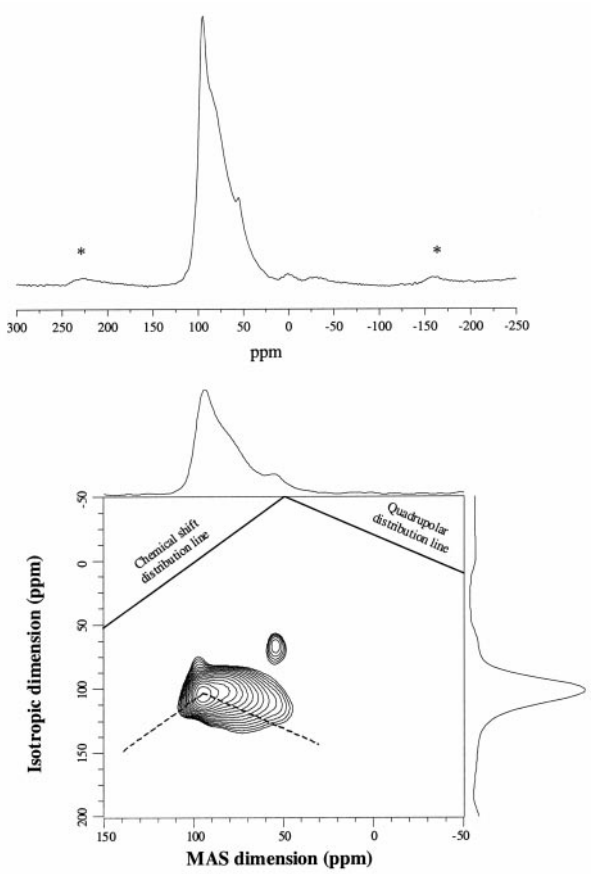

Fig. 2 Aluminium-27 1D MAS (top) and 2D 3Q MAS (bottom) NMR spectra of sample II ($Li_{1.69}Si_{9.0}Al_{3.0}O_{1.31}N_{14.69}$) recorded at $B_0 = 14.1$ T and $\nu_r = 20$ kHz. Asterisks on the 1D MAS spectrum correspond to spinning sidebands.

$\delta'_{Al} \sim 53$ ppm and a broad peak centred at ~ 83 ppm. Note that these values are the positions of peak maxima and do not correspond to the isotropic chemical shifts. A high-frequency shoulder at ~ 102 ppm is also present. The 3Q MAS NMR spectrum consists of two peaks.

Sample II: $Li_{1.69}Si_{9.0}Al_{3.0}O_{1.31}N_{14.69}$ ($m = 1.69$; $n = 1.31$)

The ^{27}Al MAS and 3Q MAS NMR spectra of sample II are displayed in Fig. 2. The 1D spectrum consists of two relatively narrow peaks, a low-intensity one at ~ 56 ppm and a dominant one at $\delta'_{Al} \sim 95$ ppm. A broad shoulder and a small peak are also present at ~ 79 and ~ 1 ppm, respectively. The 3Q MAS NMR spectrum exhibits two peaks.

Sample III: $Li_{1.0}Si_{9.5}Al_{2.5}O_{1.5}N_{14.5}$ ($m = 1.0$; $n = 1.5$)

The ^{27}Al MAS 1D NMR spectrum of this sample shows a weak peak at $\delta'_{Al} \sim -1$ ppm and a dominant broad peak at $\delta'_{Al} \sim 78$ ppm, with a narrower peak at ~ 56 ppm which is much less intense than the corresponding signal for sample I. A shoulder is also present at ~ 101 ppm. The 3Q MAS NMR spectrum contains three peaks, one of them corresponding to the 1D signal at ~ -1 ppm.

Sample IV: $Li_{2.0}Si_{8.5}Al_{3.5}O_{1.5}N_{14.5}$ ($m = 2.0$; $n = 1.5$)

The ^{27}Al MAS 1D NMR spectrum of this sample is very similar to that of sample II, though the peak at $\delta'_{Al} \sim 1$ ppm is rather stronger and that at $\delta'_{Al} \sim 55$ ppm rather weaker. Only one site appears in the ^{27}Al 3Q MAS NMR spectrum.

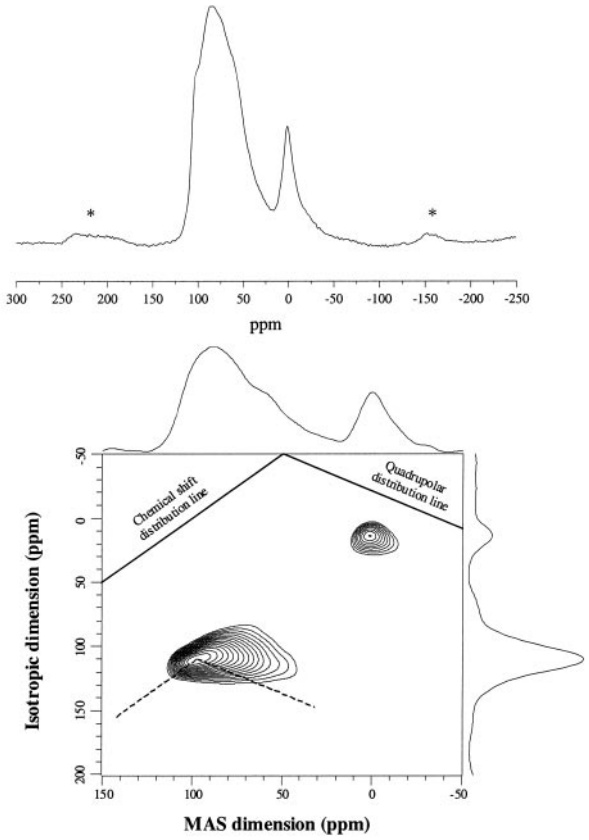

Fig. 3 Aluminium-27 1D MAS (top) and 2D 3Q MAS (bottom) NMR spectra of sample VII ($Li_{1.0}Si_{8.5}Al_{3.5}O_{2.5}N_{13.5}$) recorded at $B_0 = 14.1$ T and $\nu_r = 20$ kHz. Asterisks on the 1D MAS spectrum correspond to spinning sidebands.

Sample V: $Li_{1.0}Si_{9.0}Al_{3.0}O_{2.0}N_{14.0}$ ($m = 1.0$; $n = 2.0$)

The ^{27}Al MAS 1D NMR spectrum of this sample is similar to that of sample III, though the peak at $\delta'_{Al} \sim 3$ ppm is significantly stronger and that at ~ 57 ppm even weaker. The shoulder at ~ 101 ppm is slightly more prominent than for sample III. The 3Q MAS spectrum exhibits three peaks.

Sample VI: $Li_{2.0}Si_{7.5}Al_{4.5}O_{2.5}N_{13.5}$ ($m = 2.0$; $n = 2.5$)

Whilst the general shape of the 1D spectrum of this sample closely resembles those of samples II and IV, the signal at $\delta'_{Al} \sim 1$ ppm is significantly stronger. Three sites are resolved in the 3Q MAS spectrum.

Sample VII: $Li_{1.0}Si_{8.5}Al_{3.5}O_{2.5}N_{13.5}$ ($m = 1.0$; $n = 2.5$)

The ^{27}Al MAS and 3Q MAS NMR spectra of this sample are shown in Fig. 3. The relatively narrow peak at $\delta'_{Al} \sim 2$ ppm now has very significant intensity and there seems to be no sharp signal at ~ 53 ppm. The shape of the dominant broad peak centred at ~ 88 ppm is similar to that of sample I, with weak shoulders at ~ 60 and ~ 72 ppm. Two sites can be resolved in the 3Q MAS spectrum.

Finally, Fig. 4 shows the ^{29}Si MAS NMR spectrum of sample VII recorded at $B_0 = 7.05$ T and $\nu_r = 3.6$ kHz. This spectrum exhibits a single relatively broad peak and is representative of the ^{29}Si MAS spectra obtained for all the samples involved in this work. The observed ^{29}Si isotropic chemical shifts and linewidths are summarized in Table 2.

Discussion

All the ^{29}Si isotropic chemical shifts (Table 2) are found to lie in a very narrow range, from $\delta_{Si} = -49$ to $\delta_{Si} = -47$ ppm,

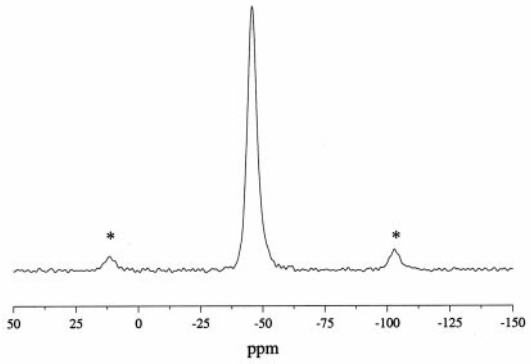

Fig. 4 Silicon-29 MAS NMR spectrum of sample VII ($Li_{1.0}Si_{8.5}Al_{3.5}O_{2.5}N_{13.5}$) recorded at $B_0 = 7.05$ T and $\nu_r = 3.6$ kHz. An exponential line broadening function of 100 Hz was applied prior to Fourier transformation. Asterisks correspond to spinning sidebands.

indicating that the silicon environments in all of these phases are electronically similar. Linewidths are found to lie in the range 250–350 Hz (though this includes the 100 Hz line broadening) and no obvious correlation with the content in nitrogen or aluminium can be found, as was previously shown for β-sialons.[11] The ^{29}Si isotropic chemical shifts are very close to those observed for β-Si_3N_4,[28] β-sialon,[7] polytypoids 21R,[9] 15R[8,9] and several compositions of α-sialon stabilized by Ca and Y.[29] They are also very close to those reported for the two silicon positions in α-Si_3N_4,[28] O-sialons[30] and 12H polytypoid.[8] In fact, it is accepted that silicon is coordinated by four nitrogen atoms in the latter phase.[7,29] An alternative explanation[29] is that the chemical shift remains unaltered, even though the composition of the $SiN_{4-x}O_x$ ($x = 0$–4) tetrahedra in the structure changes, as a consequence of the nature of isomorphous substitution, *i.e.* an Al–O unit replaces an isoelectronic Si–N unit, since the groups have similar electronegativities[31] and, thus, only very small changes in the electron distribution over atomic orbitals of importance to the isotropic chemical shifts are expected. However, the ^{29}Si isotropic chemical shifts for the complete range $SiN_{4-x}O_x$ ($x = 0$–4) have been previously obtained[5] and, although some overlap of the chemical shift ranges from different tetrahedral units occurs, it is normally possible to differentiate distinct environments. It is quite likely therefore that the majority of silicon atoms are in an SiN_4 coordination in all the Li α-sialon samples involved in this work, confirming the general preference for silicon to bond to nitrogen. However, small amounts of SiN_3O environments cannot be excluded. The α-sialon unit cell contains two types of silicon site, as for α-Si_3N_4. Unfortunately the ^{29}Si linewidths we observe (4–6 ppm) obscure the expected signal splitting (1.9 ppm in α-Si_3N_4 [28]) so we are unable to tell if Al substitution occurs preferentially at one of the sites, though this might conceivably account for the apparent small variation in our values of δ_{Si}. Increasing content of Li seems to cause the ^{29}Si line to become broader,

Table 2 Silicon-29 isotropic chemical shifts and linewidths for the Li α-sialon samples

Sample	Compound	δ_{Si}/ppm[a]	fwhh[b]/Hz
I	$Li_{1.3}Si_{9.5}Al_{2.5}O_{1.2}N_{14.8}$	−47	260
II	$Li_{1.69}Si_{9.0}Al_{3.0}O_{1.31}N_{14.69}$	−47	320
III	$Li_{1.0}Si_{9.5}Al_{2.5}O_{1.5}N_{14.5}$	−48	250
IV	$Li_{2.0}Si_{8.5}Al_{3.5}O_{1.5}N_{14.5}$	−49	330
V	$Li_{1.0}Si_{9.0}Al_{3.0}O_{2.0}N_{14.0}$	−47	250
VI	$Li_{2.0}Si_{7.5}Al_{4.5}O_{2.5}N_{13.5}$	−48	350
VII	$Li_{1.0}Si_{8.5}Al_{3.5}O_{2.5}N_{13.5}$	−47	260

[a]Estimated to be accurate to ±2 ppm. [b]Full width at half-height, estimated to be accurate to *ca.* +10 Hz. However, these values include a superimposed 100 Hz line broadening function.

probably because of an increase in disorder in the structure. This result means that, because of stoichiometric constraints, aluminium is expected to have a range of tetrahedral coordinations, $AlN_{4-x}O_x$ ($x=0$–4).

As the content in oxygen increases, the ^{27}Al 1D MAS spectra show distinct changes in the relative intensities and the shapes of the peaks, while the actual peak positions remain almost constant (Table 1). The well-separated shift ranges of AlO_4 and AlO_6 units usually allow rapid identification of the coordinations present in a given phase. All the ^{27}Al MAS spectra except that shown in Fig. 1 exhibit a relatively broad peak in the range -1 to $+3$ ppm (note that this corresponds to the positions of peak maxima and not to isotropic chemical shifts) which can be unambiguously attributed to AlO_6 octahedra. The corresponding NMR parameters are given in Table 1. The isotropic chemical shifts are found to lie between $\delta_{Al}=3$ ppm and $\delta_{Al}=9$ ppm. The second-order quadrupolar effect parameters are found to be in the range $\lambda=1.9$–2.6 MHz. As previously mentioned, they give good estimates of the quadrupolar coupling constants $|\chi|$. These are relatively small, as expected for aluminium in AlO_6 environments. Detailed inspection of Figs. 1–3 (and the Al spectra of the other samples) shows that the intensity of the peak corresponding to AlO_6 octahedra generally increases with increasing oxygen content. It should be emphasized that this corresponds to a relatively small amount of AlO_6, even for the sample having the highest content in oxygen. Furthermore, a small amount of Li–Si–Al–O–N glass may remain in the materials.[18] These facts suggest that this peak is likely to arise from the glassy components. The implication of this observation is that with increasing oxygen content there is a tendency for the glassy components to resist crystallization.

The one-dimensional ^{27}Al spectra show similar characteristics in their bandshapes in the four-coordinate region. Generally, there is a broad band at $\delta'_{Al}=ca.$ 84–94 ppm with sharper peaks or shoulders to high ($\sim$100 ppm) and to low frequency ($\delta'_{Al}=53$–55 ppm). However, there are distinct differences in the intensity distribution between the spectra. Thus, the Al spectra of samples II, IV and VI are closely comparable in that the high-frequency peak is prominent whereas the low-frequency signal is weak. For samples I, III, and V, on the other hand, the reverse is the case. Both signals are very weak or absent in Fig. 3. In all cases (especially for samples I, III, V and VII) the majority of the intensity lies between the sharper peaks, which are apparent largely because of their sharpness. These sharper signals clearly relate to ^{27}Al environments which are relatively symmetric and may be assigned to AlO_4 (low frequency) and AlN_4 (high frequency) sites on the grounds of their chemical shifts (though it should be recognised that lack of precise tetrahedral symmetry arising from more remote substituents and/or low crystallographic site symmetry may even for AlO_4 and AlN_4 environments lead to substantial electric field gradients). Their sharpness also suggests that the signals arise from crystalline domains. The broad central signal in the four-coordinate region presumably arises from the mixed environments AlO_3N, AlO_2N_2 and $AlON_3$. These are expected to have higher nuclear quadrupole coupling constants and therefore to give broad overlapping bands with unresolved second-order features.

Previous ^{27}Al MAS NMR studies of nitrogen ceramics reported a relatively narrow resonance at $\delta'_{Al}\sim110$ ppm, and this peak has been assigned by comparison with AlN to AlN_4 coordination.[6,8] Also, Smith has studied a series of β′-sialons, $Si_{6-z}Al_zO_zN_{8-z}$ with $z=1$, 2 and 4, by ^{27}Al 1D MAS NMR.[16] The peaks at $\delta'_{Al}\sim68$ and ~89 ppm in the spectrum of the $z=4$ sample were assigned to AlO_4 and AlO_2N_2 units while those at $\delta'_{Al}\sim75$ and ~108 ppm in the spectrum of the $z=1$ sample were attributed to AlO_3N and AlN_4 coordinations, respectively. In view of the fact that the high-frequency peak maximum seen for samples II, IV and VI is only at $\delta'_{Al}\sim100$ ppm, we cannot be sure this represents AlN_4 environments, but there is no reason to suppose $AlON_3$ would have the lower quadrupole coupling constant implied by the relative sharpness of the signal observed.

Because of the variations of bandwidth and bandshape of the various peaks obtained in the present work (and of the existence of spinning sidebands), it is not feasible to extract quantitative or even semi-quantitative information of relative intensities. However, the qualitative features are clear. The AlN_4 site has substantial intensity when m is high, *i.e.* the Li : (Si + Al) ratio is high. This correlates with a high ratio of N : Si (between 1.63 and 1.80) so that satisfying the preference of Si for N is easy, leaving substantial amounts of nitrogen to coordinate to Al. Correspondingly, the AlO_4 peak is very weak for these samples. We have no explanation as to why the AlO_4 intensity is markedly higher in Fig. 1 than for any other sample.

When N : Si is low (between 1.53 and 1.59), on the other hand, the AlN_4 signal only appears as a shoulder, whereas the AlO_4 peak is more prominent. The exception to the latter situation is Fig. 3, and it is probably significant that in this case the N : Si ratio (1.59) is the highest in the group, as is the intensity in the AlO_6 signal.

The one-dimensional ^{27}Al spectra therefore clearly reveal the changing nature of the aluminium environment as the sample composition is varied. The conclusions are strengthened and confirmed by the two-dimensional spectra. Samples I, II, III, V and VI show 2D signals assigned to AlO_4 environments. The NMR parameters were derived using eqns. (1) and (2), and are given in Table 1. The isotropic chemical shifts are found to lie between $\delta_{Al}=56$ ppm and $\delta_{Al}=60$ ppm. The second-order quadrupolar effect parameters are, as expected, modest in magnitude for this signal, being in the range 1.2–2.5 MHz.

The more intense 2D peak does not allow any distinction to be made between AlO_3N, AlO_2N_2, $AlON_3$ and AlN_4 units, even at the high magnetic field used. Some average NMR parameters may be derived and are reported in Table 1. The isotropic chemical shifts thus obtained are all in the range $\delta_{Al}=96$ ppm to $\delta_{Al}=98$ ppm, except for $Li_{1.0}Si_{8.5}Al_{3.5}O_{2.5}N_{13.5}$, for which the shift is unaccountably higher ($\delta_{Al}=103$ ppm). The second-order quadrupolar effect parameters are in the range 2.1–3.3 MHz, in general higher than for the AlO_6 and AlO_4 sites, as expected, and notably so for samples lacking a strong high-frequency 1D peak (the exception in this case being sample V).

It has been suggested,[11,16] that ^{27}Al spectra of sialons are consistent with a model in which distinct (Si,N) and (Al,O) micro-domains exist, the (Si,N) one becoming smaller and the (Al,O) one becoming larger when the aluminium and oxygen contents are increasing. At low aluminium and oxygen contents the small (Al,O) regions would result in virtually all aluminium being close to the interface, so that the majority of aluminium coordinations will be mixed. When the aluminium and oxygen contents increase, the majority of aluminium coordinations may still be mixed and the relative intensity of the peak due to AlO_4 units will increase compared to that of the peaks attributed to aluminium tetrahedral mixed units. Although we cannot resolve separate signals from such mixed units, we believe our results are consistent with the presence of a range of Al environments in each case, with concentrations varying as sample composition changes.

The characteristic lines for pure distribution of the efg tensor and the isotropic chemical shift are drawn on the 3Q MAS spectra.[32,33] A detailed inspection of the 2D 3Q MAS NMR spectra of samples I (Fig. 1), III, V and VII (Fig. 3) reveals that the main peak appears to have a trend in the general direction of the distribution line for isotropic chemical shifts. This distribution will result in a significant broadening of the ^{27}Al 1D MAS NMR spectra due to the range of isotropic chemical shifts generated. In the other cases, the peak is sharper and shows some evidence of a small distribution in both isotropic

chemical shifts and efg tensor components, as can be seen for samples II (Fig. 2), IV and VI. The peaks tend to run parallel to the chemical shift distribution line at the high-frequency side, indicating a small distribution in isotropic chemical shifts. At the low-frequency side they bend away in the quadrupolar distribution line direction, reflecting a small distribution in efg tensor components. The reason for these observations is not clear. They may relate to the inherent disorder in the structure. It is well known that both atomic and structural disorder can occur in sialons,[34] though XRD clearly confirms the samples to be crystalline. A variation in the proportions of the different Al environments is probably responsible.

Conclusions

The effect of (Al,O) substitution for (Si,N) on the structure of Li α-sialon ceramics has been studied using ^{29}Si and ^{27}Al MAS NMR. The ^{29}Si resonance showed very little change across the whole substitution range. The invariant peak position at $\delta_{Si} \approx -48$ ppm suggests that SiN_4 units form the preferred environment at all compositions. This result means that aluminium is expected to have a range of tetrahedral coordinations, $AlN_{4-x}O_x$ ($x=0$–4), and confirms the general preference for silicon to bond to nitrogen.

The ^{27}Al 1D MAS NMR spectra show the presence of a small octahedral AlO_6 peak across most of the substitution range. This peak is likely to be arising from the glassy components. A range of tetrahedral coordinations is observed, including a distinct signal for AlO_4, a broad band for $AlO_3N+AlO_2N_2+AlON_3$ and a sharper high-frequency signal for AlN_4 (or possibly $AlON_3$). The AlO_4 peak tends to be prominent for low N : Si ratios whereas the AlN_4 resonance is of higher intensity when the N : Si ratio is high, leaving more nitrogen to coordinate to aluminium. These results confirm the general preference for nitrogen to bond to silicon and for oxygen to coordinate to aluminium. Two-dimensional MQMAS spectra confirm these conclusions and produce some data on true Al chemical shifts and quadrupolar effect parameters. However, the results show that, although the MQMAS NMR technique does not allow the different aluminium tetrahedral units with mixed N,O coordination to be resolved, the ^{27}Al spectra of lithium α-sialons have considerable value in monitoring the changes from more nitrogen-rich to more oxygen-rich $Al(O,N)_4$ environments as the N : O ratio in the starting composition is varied.

Acknowledgements

We thank EPSRC for funding under the JREI programme (grant GR/L24250) which allowed the purchase of the 600 MHz spectrometer and for a postdoctoral fellowship to one of us (P. K.) under grant GR/M88341. We are also grateful to R. Dupree, M.E. Smith and A.P. Howes for advice and assistance with spectrometer operation.

References

1 Y. Oyama and O. Kamigaito, *Jpn. J. Appl. Phys.*, 1971, **10**, 1637.
2 K. H. Jack and W. I. Wilson, *Nature Phys. Sci.*, 1972, **238**, 28.
3 K. H. Jack, *J. Mater. Sci.*, 1976, **11**, 1135.
4 S. Hampshire, H. K. Park, D. P. Thompson and K. H. Jack, *Nature*, 1978, **274**, 880.
5 R. Dupree, M. H. Lewis and M. E. Smith, *J. Am. Chem. Soc.*, 1988, **110**, 1083.
6 N. D. Butler, R. Dupree and M. H. Lewis, *J. Mater. Sci. Lett.*, 1984, **3**, 469.
7 R. Dupree, M. H. Lewis, G. Leng-Ward and D. S. Williams, *J. Mater. Sci. Lett.*, 1985, **4**, 393.
8 J. Klinowski, J. M. Thomas, D. P. Thompson, P. Korgul, K. H. Jack, C. A. Fyfe and G. C. Gobbi, *Polyhedron*, 1984, **3**, 1767.
9 G. L. Marshall, R. K. Harris, D. Apperley and R. Yeung, *Proc. Symp. Sci. Ceram.*, 1987, **14**, 347.
10 I. E. Farnan, R. Dupree, A. J. Forty, Y. S. Jeong, G. E. Thompson and G. C. Wood, *Philos. Mag. Lett.*, 1989, **4**, 189.
11 R. Dupree, M. H. Lewis and M. E. Smith, *J. Appl. Crystallogr.*, 1988, **21**, 109.
12 R. Dupree, M. H. Lewis and M. E. Smith, *J. Am. Chem. Soc.*, 1989, **111**, 5125.
13 K. R. Carduner, R. O. Carter, M. J. Rokosz, C. Peters, G. M. Crosbie and E. D. Stiles, *Chem. Mater.*, 1989, **1**, 302.
14 R. K. Harris, M. J. Leach and D. P. Thompson, *Chem Mater.*, 1989, **1**, 336.
15 J. Haase, D. Freude, T. Frohlich, C. Himpel, F. Kerke, E. Lippmaa, P. Pfeifer, P. Sarv, H. Schafer and B. Seiffert, *Chem. Phys. Lett.*, 1989, **156**, 328.
16 M. E. Smith, *J. Phys. Chem.*, 1992, **96**, 1444.
17 L. Frydman and J. S. Harwood, *J. Am. Chem. Soc.*, 1995, **117**, 5367.
18 Z. B. Yu, D. P. Thompson and A. R. Bhatti, *Br. Ceram. Trans.*, 1998, **97**, 41.
19 S. P. Brown and S. Wimperis, *J. Magn. Reson.*, 1997, **124**, 279.
20 S. P. Brown and S. Wimperis, *J. Magn. Reson.*, 1997, **128**, 42.
21 J. P. Amoureux and C. Fernandez, *Solid State Nucl. Magn. Reson.*, 1998, **10**, 211.
22 C. Fernandez, J. P. Amoureux, J. M. Chezeau, L. Delmotte and H. Kessler, *Microporous Mater.*, 1996, **6**, 331.
23 M. Hunger, P. Sarv and A. Samoson, *Solid State Nucl. Magn. Reson.*, 1997, **9**, 115.
24 C. Fernandez and J. P. Amoureux, *Chem. Phys. Lett.*, 1995, **242**, 449.
25 P. P. Man, *Phys. Rev. B*, 1998, **58**, 2764.
26 D. Massiot, B. Touzo, D. Trumeau, J. P. Coutures, J. Virlet, P. Florian and P. J. Grandinetti, *Solid State Nucl. Magn. Reson.*, 1996, **6**, 73.
27 P. Faucon, T. Charpentier, D. Bertrandie, A. Nonat, J. Virlet and J. C. Petit, *Inorg. Chem.*, 1998, **37**, 3726.
28 R. K. Harris, M. J. Leach and D. P. Thompson, *Chem. Mater.*, 1990, **2**, 320.
29 M. J. Leach, Thesis, University of Durham, 1990.
30 J. Sjöberg, R. K. Harris and D. C. Apperley, *J. Mater. Chem.*, 1992, **2**, 433.
31 N. Janes and E. Oldfield, *J. Am. Chem. Soc.*, 1985, **107**, 6769.
32 P. R. Bodart, *J. Magn. Reson.*, 1998, **133**, 207.
33 D. Freude, *Encyclopaedia of Analytical Chemistry*, ed. R. A. Meyers, John Wiley & Sons, Chichester, 2000, pp. 12188–12224.
34 A. Nordmann, Y. B. Cheng and M. E. Smith, *Chem. Mater.*, 1996, **8**, 2516.